Supporting Information for:

New insights into solvent-induced structural changes of ^{13}C labelled metal-organic frameworks by solid state NMR

Marcus Rauche[a†], Sebastian Ehrling[b†], Simon Krause[b], Irena Senkovska[b], Stefan Kaskel[b], Eike Brunner[a]*

[a] Chair of Bioanalytical Chemistry, TU Dresden, D-01062 Dresden, Germany.

[b] Chair of Inorganic Chemistry, TU Dresden, D-01062 Dresden, Germany.

[†] Both authors contributed equally.

Corresponding author
Eike Brunner Chair of Bioanalytical Chemistry, TU Dresden, D-01062 Dresden, Germany E-mail: eike.brunner@tu-dresden.de Fax: +49 351 46337188; Tel: +49 351 463 32631

Table of content

1. Experimental details

Materials. Ni(NO$_3$)$_2$·6H$_2$O (98 %), 2,6-H$_2$ndc, dabco (99%) and 2,6-dibromenaphtalene (97%) were purchased from Sigma Aldrich. ^{13}C-enriched CO$_2$ was purchased from Eurisotop (99.3% ^{13}C enrichment). 2,6-naphtalenedicarboxylic-d6 acid and 1,4-diazabicyclo[2.2.2]octane-d12 were purchased from CDN ISOTOPES. Both compounds have at least 98% deuterium content. All solvents were at least of analytical grade, purchased from commercial suppliers and used without further purification.

Synthesis of 2,6-H$_2$ndc: 2,6-Dibromonaphtalene (5.0 g, 17.5 mmol, 1 eq.) was dissolved in 150 mL THF (SPS) in a Schlenk-flask under continuous stirring. The solution was cooled down to -78 °C with a cooling bath (EtOH / N$_{2,lq.}$). For lithiation, 15.9 mL n-BuLi (2.5 M in hexane, 2.15 eq.) was slowly dripped over a period of 45 minutes. After that, the solution was stirred at -78 °C for a further 30 minutes, resulting in turbidity. After the suspension has been heated to room temperature, ^{13}C marked CO$_2$ was passed over the suspension to achieve carboxylation. The flask was left under slight over-pressure for 12 h. To work-up the reaction, a drop of H$_2$O was added to deactivate any unreacted n-BuLi. The solvent was then completely removed by the rotary evaporator. The resulting white solid was dissolved in water and sucked off via a G5 frit. The filtrate was adjusted with 20 mL 2 N HCl to a pH value of 1 to precipitate the product. The resulting white solid was sucked off, washed again with a small amount of H$_2$O and acetone, and dried overnight in an oven at 85 °C. Yield: (84% with respect to 2,6-dibromonaphtalene). The purity was determined using ^{1}H NMR, ^{13}C NMR and ESI-MS.

Synthesis of 1: Typically, Ni(NO$_3$)$_2$·6H$_2$O (407 mg, 1.4 mmol, 1.56 eq.) was dissolved in 5 mL DMF, ^{13}C-2,6-H$_2$ndc (306 mg, 1.4 mmol, 1.56 eq.) was dissolved in 15 mL DMF, and dabco (100 mg, 0.89 mmol) was dissolved in 5 mL MeOH. The three resulting solutions are combined in a Teflon vessel (50 mL) and heated in an autoclave at 120 °C for 48 h. The resulting dark green crystals were filtered and washed with DMF several times. A part of the sample was soaked in DCM and the supernatant solution was replaced several times in the first two hours. After two days the crystals were filtered off in an argon flow and the solvent was removed under reduced pressure over night. During solvent removal the colour changed from dark green to dark yellow.

Synthesis of 2. Typically, 2,6-H$_2$ndc (298.9 mg, 1.37 mmol) was dissolved in 30 mL DMF. To the clear linker solution, Ni(NO$_3$)$_2$·6H$_2$O (296 mg, 1.5 mmol, 1.1 eq.) was added. Finally, dabco (337 mg, 3 mmol, 2.2 eq.) was added whereby the solution immediately turned cloudy. The resulting mixture was then treated in the ultra-sonic bath for 60 minutes increasing the suspension temperature from 25 °C to 55 °C. The mother solution was removed by centrifugation and the resulting particles were washed several times with DMF. A part of the sample was soaked in DCM and the supernatant solution was replaced several times in the first two hours. After two days the crystals were filtered in an argon flow and the solvent was removed under reduced pressure and 150 °C over night. During solvent removal no colour changed was observed, meaning the crystals remained their green colour.

Synthesis of deuterated analogue (samples 3, 4, 5). The molar ratio of starting materials and the work-up procedure of the resulting crystals were kept like described above for the synthesis of **1**. However, the amount of reactants was drastically decreased due to the high cost of the deuterated compounds. The sample naming and the exact synthesis parameters are given in Table S1 and Table S2 respectively.

Table S1. Selectively deuterated DUT-8(Ni) compounds.

Identifier	Sample name	Used linker	Used pillar
3	flexible "d^6-DUT-8"	^{2}H-2,6-H$_2$ndc	^{1}H-dabco
4	flexible "d^{12}-DUT-8"	2,6-H$_2$ndc	d^{12}-dabco
5	flexible "d^{18}-DUT-8"	d^6-2,6-H$_2$ndc	d^{12}-dabco

Table S2. Synthesis parameters of the selective deuterated DUT-8(Ni) derivate.

Compound	m(Ni(NO$_3$)$_2$·6H$_2$O) / solvent	Respective linker / solvent	Respective pillar / solvent
3	65.4 mg / 1.4 mL DMF	50 mg / 3 mL DMF	16 mg / 1.1 mL MeOH
4	65.4 mg / 1.4 mL DMF	48.6 mg / 3 mL DMF	17.8 mg / 1.1 mL MeOH
5	65.4 mg / 1.4 mL DMF	50 mg / 3 mL DMF	17.8 mg / 1.1 mL MeOH

Solvent exchange. Directly after the synthesis the resulting particles of **1** and **2** were washed with fresh DMF to remove unreacted chemicals. Then the crystals of **1** were exchanged to a bunch of different solvents covering polar and non-polar solvents. All polar solvents were exchanged directly from DMF. To obtain the samples containing non-polar solvents, in contrast, DMF was firstly exchanged to DCM, due to the low miscibility of DMF and the used saturated *n*-alkanes. DMF was removed by decantation and the crystals were suspended in the respective fresh solvent. The supernatant solution was removed several times in the first 2 hours and then every 12 hours for another 2 days.

Characterization. Powder X-ray diffraction (PXRD) experiments at room temperature were carried out using STOE STADI P diffractometer using Cu-Kα1 radiation (λ = 1.5405 Å) and a 2D detector (Mythen, Dectris) in transmission geometry. For nitrogen adsorption at 77 K Belsorp-Max from MicrotracBEL Corp. (Japan) was used. Prior to the measurements, the samples were desolvated in dynamic vacuum at room temperature for at least 16 hours. ^{1}H and ^{13}C NMR measurements of ^{13}C labelled 2,6-H_2ndc were carried out using a Bruker DRX 500 P spectrometer. ^{1}H and ^{13}C MAS NMR spectroscopy was carried out using a BRUKER Ascend 800 and a BRUKER Avance 300 spectrometer at room temperature. The solvent free samples were transferred into a 2.5 mm zirconium rotor in an argon-filled glovebox. Spectra were recorded at a resonance frequency of 800.19 MHz for ^{1}H and 201.26 MHz for ^{13}C using a triple-resonance 2.5 mm MAS NMR probe and a sample spinning rate of 15 kHz. Ramped ^{1}H-^{13}C cross polarization (CP) with SPINAL 64 proton decoupling during signal acquisition were applied. The chemical shifts were referenced to Adamantane. (300.13 MHz for ^{1}H and 75.47 MHz for ^{13}C using a 2.5 mm double resonance probe at a MAS frequency of 15 kHz.) Respective ESI-MS spectra were acquired through direct infusion of 1μl at 0.2 μl min^{-1} flow rate in a Q-TOF 6538 UHD mass spectrometer (Agilent Technology, Santa Clara, CA, U.S.A.), equipped with a DuoSpray® interface operating with an ESI probe. The ESI source parameters were optimized and were as follows: negative polarity, Ionspray Voltage Floating 3500 V, Temperature 250 °C, Declustering Potential (DP) 110 V, Skimmer 45 V, Collision Energy (CE) 10 V.

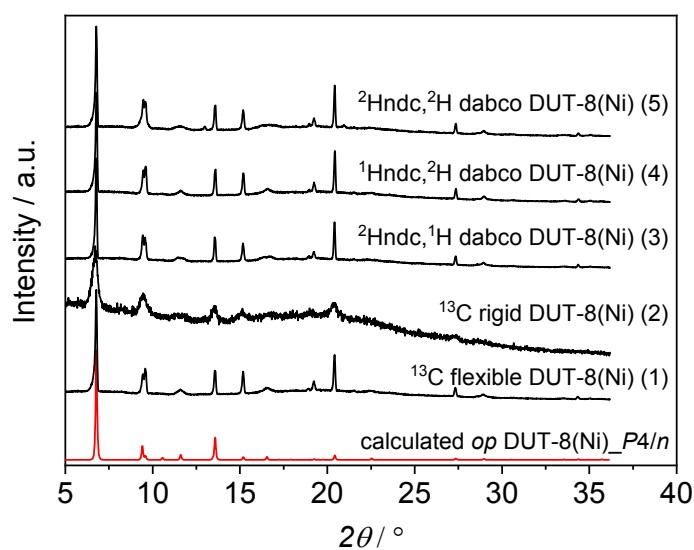## 2. Powder X-ray diffraction (PXRD) patterns of synthesized MOFs

Figure S1. PXRD of all DUT-8(Ni) samples (compounds **1**-**5**) after the synthesis, solvated in DMF.
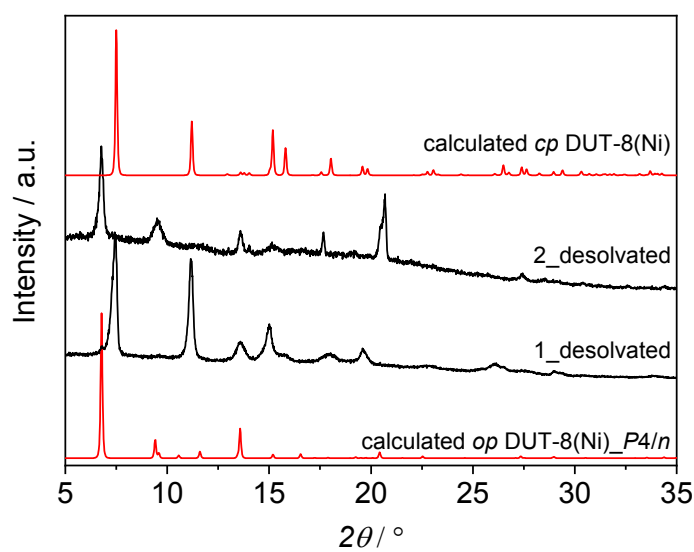

Figure S2. PXRD of compounds **1** and **2** after solvent removal and calculated diffractograms for the *op* and *cp* state.
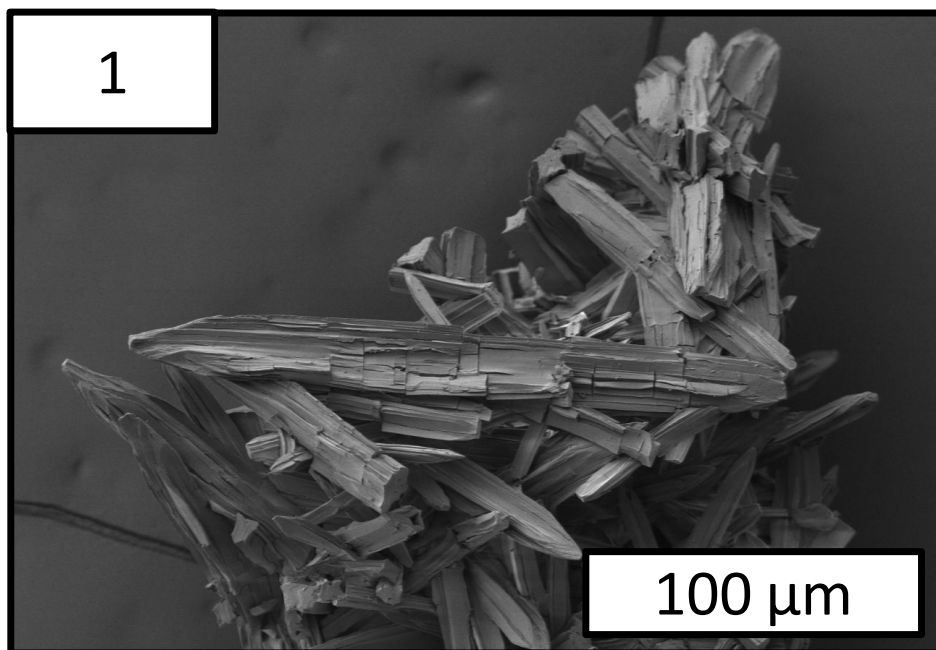
1

100 μm

Figure S3. SEM images of compounds **1** and **2** after desolvation.
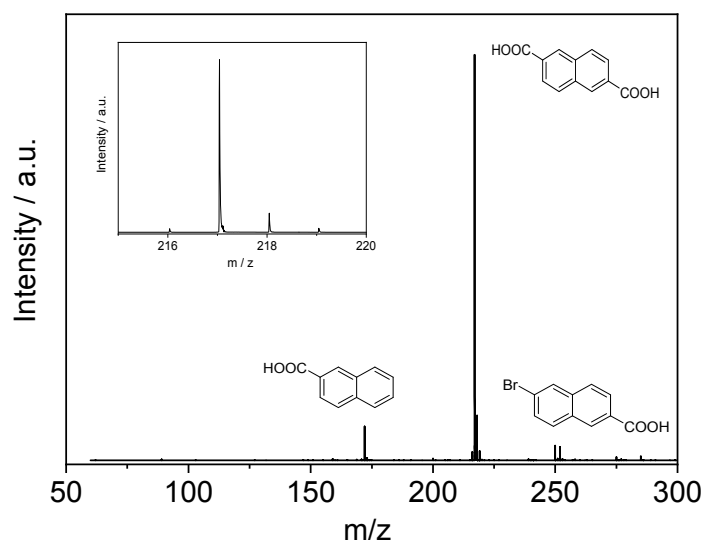
3. SEM images

4. Linker characterization

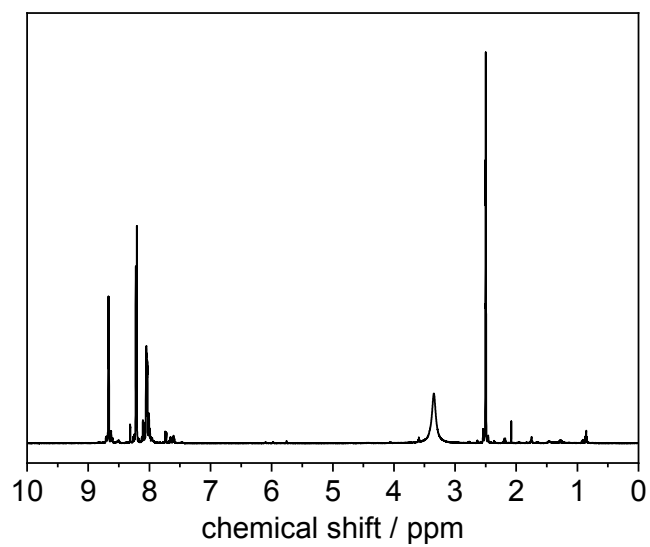Figure S4. ESI MS spectra of the ^{13}C labelled 2,6-H_2ndc dissolved in MeOH.

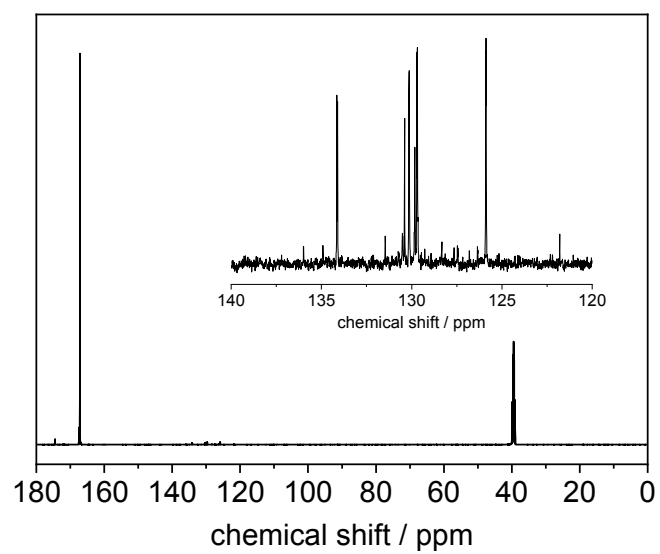Figure S5. ^{1}H NMR of ^{13}C labelled 2,6-H_2ndc in DMSO-d^{6}.

Figure S6. ^{13}C NMR of ^{13}C labelled 2,6-H$_2$ndc in DMSO-d^6.

5. Field-dependent NMR experiments

Assignment of the ^{13}C CP MAS NMR spectrum of DUT-8(Ni)

The ^{13}C CP MAS NMR spectrum of DUT-8(Ni) synthesized with ^{13}C-labelled carboxylates in the 2,6-ndc linkers is dominated by the ^{13}C signal of the carboxylate groups (cf. Figure 1). It exhibits, however, further signals due to ^{13}C nuclei in components with natural abundance which are assigned in Figure S7 below.
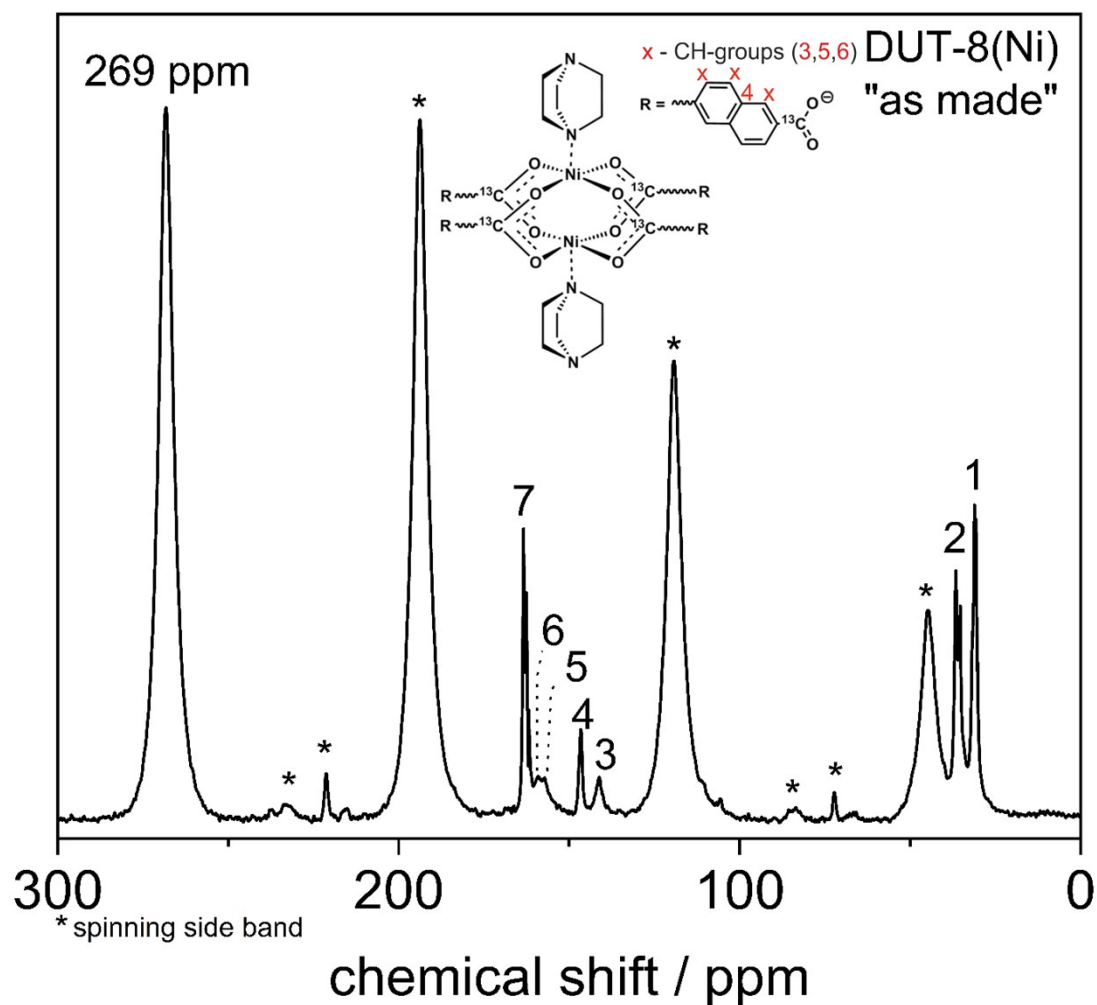

Figure S7. ^{13}C CP MAS NMR spectrum of compound **1** along with the complete signal assignment as provided in the insert. Signal 1,2 and 7 can be assign to DMF.

Magnetic field dependence of the ^{13}C NMR linewidth of linker carboxylates

The static ^{13}C NMR line width of linker carboxylates is reflected by the intensities of the spinning sidebands.[1] In order to discriminate between possible line broadening interactions, the spinning sideband pattern was measured at two different magnetic field strengths corresponding to 300 and 800 MHz ^{1}H resonance frequency. The second moments M_2 were then analysed as specified below. As can be seen from Figures S8 and S9, the second moment is field-dependent. Calculation of M_2 according to eq. (3) explained below yields the values provided in Figure S9. The ratio between the values measured at field strengths corresponding to 800 and 300 MHz ^{1}H resonance frequency is 6.7 and agrees well with the expected ratio of 7.1 for line broadening proportional to B_0^2 (see below).
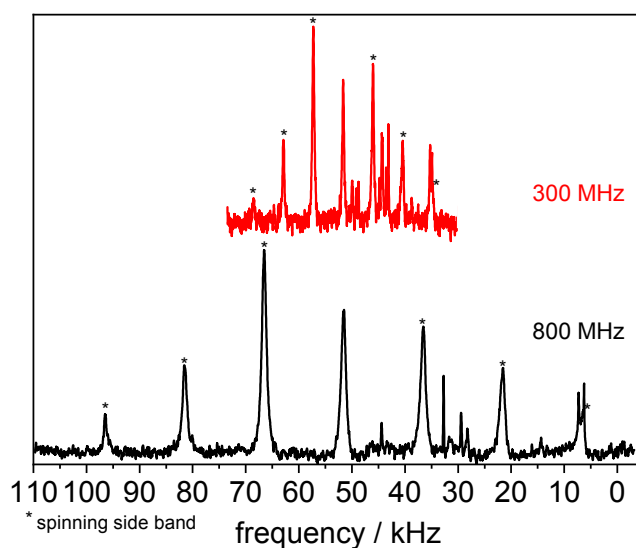

Figure S8. ^{13}C CP MAS NMR spectra of compound **1** measured at different magnetic field strengths plotted as a function of frequency. The measurements were carried out at magnetic fields corresponding to 300 and 800 MHz ^{1}H resonance frequency, respectively.
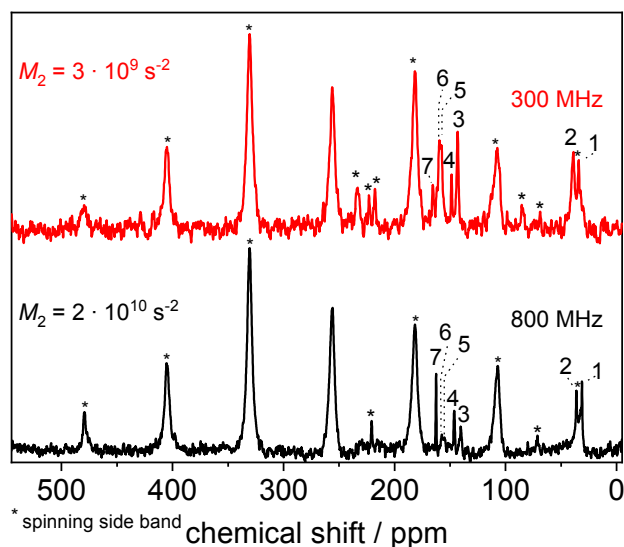

Figure S9. ^{13}C CP MAS NMR spectra of compound **1** measured at different magnetic field strengths plotted as a function of chemical shift. Signal assignment is provided in Figure S7.

Second moment M_2

The total 2nd moment M_2 is the sum of the contributions of various line broadening interactions. Note, that both, the contributions of CSA and electron-nucleus interactions to M_2 are proportional to B_0^2 (see below).

Line broadening interactions relevant for this work:

1) Chemical shift anisotropy[1]

$$M_2^{CSA} = \frac{4}{45}\gamma_I^2 B_0^2 \Delta\delta^2 (1 + \frac{1}{3}\eta^2)$$ (1)

γ_I: magnetogyric ratio
B_0:   induction of the magnetic field
$\Delta\delta$:   chemical shift anisotropy of CSA tensor
η: asymmetry parameter of CSA tensor

2) Electron-nucleus dipolar interactions[2,3]

$$M_2^{en} = \frac{4}{5}\left(\frac{\mu_o}{4\pi}\gamma_I \mu_e\right)^2 \sim (B_0)^2$$ (2)

μ_0:   vacuum permeability
μ_e: averaged electron magnetic moment, which is proportional to B_0

Calculation of M_2 from spinning sideband patterns of MAS NMR signals[1]

$$M_2 = 4\pi^2 v_r^2 \frac{\sum_{n=-\infty}^{\infty} n^2 I_n}{\sum_{n=-\infty}^{\infty} I_n}$$ (3)

v_r: sample spinning rate in Hz
n: spinning side band number
I_n: intensity of nth spinning sideband

6. Temperature-dependent NMR experiments

Magnetization measurements revealed volume susceptibilities of the order of $10^{-5} \ldots 10^{-4}$ for DUT-8(Ni).[4] Typical paramagnetic solids exhibit volume susceptibilities in the range of $10^{-3} \ldots 10^{-2}$, i.e., two orders of magnitude higher values. This supports the idea of antiferromagnetic coupling in the Ni-Ni paddle wheels as explained in main text (page 2). In order to further substantiate this conclusion, temperature-dependent ^{13}C NMR experiments were carried out. If the observed high isotropic chemical shift would be caused by paramagnetism, it should decrease with increasing temperature according to the Curie law. The opposite is, however, observed (see Figure S10). This further supports our conclusion that the nickel atoms in the paddle wheels are antiferromagnetically coupled.

It should also be noted that the residual linewidth of the ^{13}C CP MAS NMR signal of linker carboxylates is considerably larger for the rigid variant than for the flexible one (see Figure S11). Moreover, it is temperature-independent pointing towards static disorder such as due to defects in rigid DUT-8(Ni).

Table S3. Temperature dependence of the ^{13}C chemical shift of compound **1**.

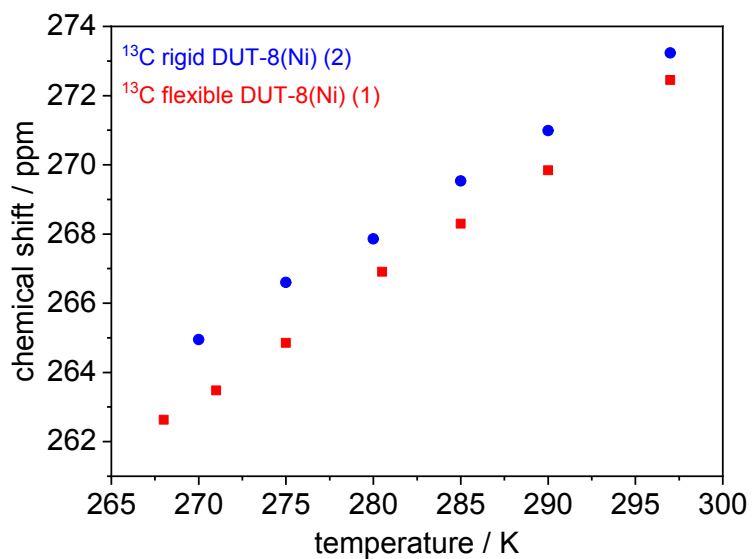| Temperature / K	Chemical shift / ppm
297	272.45
290	269.84
285	268.30
280	266.91
275	264.85
271	263.48
268	262.63

Figure S10. Temperature dependence of the chemical shift of the carboxylate ^{13}C CP MAS NMR signal of compounds **1** (red) and **2** (blue).
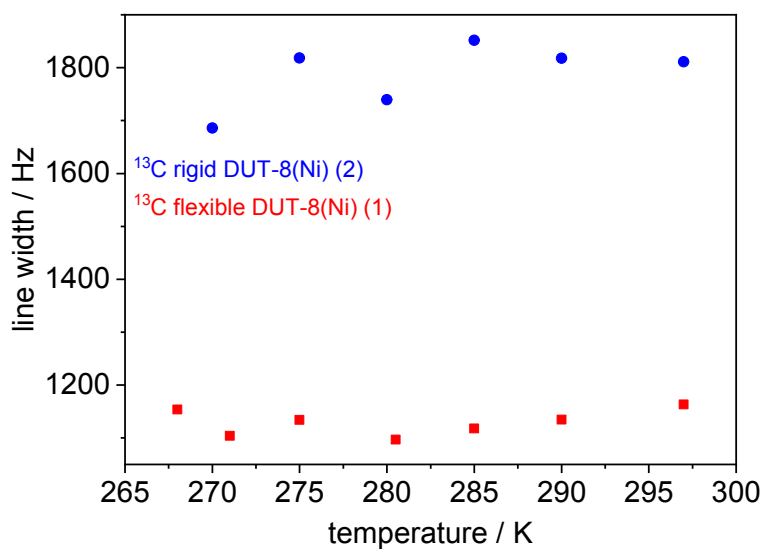

Figure S11. Temperature dependence of the residual line width of the carboxylate ^{13}C CP MAS NMR signal of compounds **1** (red) and **2** (blue).

7. Solvent effects

The solvent influence upon the ^{13}C and ^{1}H solid-state NMR spectra was studied for a series of solvents of different polarity (see Table S4).

Table S4. ^{13}C and ^{1}H NMR chemical shifts obtained for DUT-8(Ni) synthesized with selectively ^{13}C labelled 2,6-H_2ndc linker soaked in different organic solvents of different polarity.

Solvent	Relative polarity[5]	[13]C chemical shift	[1]H chemical shift signal A	[1]H chemical shift signal B
DMF	0.386	269 ppm	9.65 ppm	13.13 ppm
NMP	0.355	263 ppm	9.56 ppm	12.85 ppm
DCM	0.309	260 ppm	9.48 ppm	12.53 ppm
Toluene	0.099	251 ppm	10.01 ppm	
n-heptane	0.012	237 ppm	9.77 ppm	
n-hexane	0.009	234 ppm	9.63 ppm	
n-hentane	0.009	230 ppm	9.03 ppm	

A pronounced dependence of the ^{13}C chemical shift on the solvent polarity is observed (cf. Figure S12).
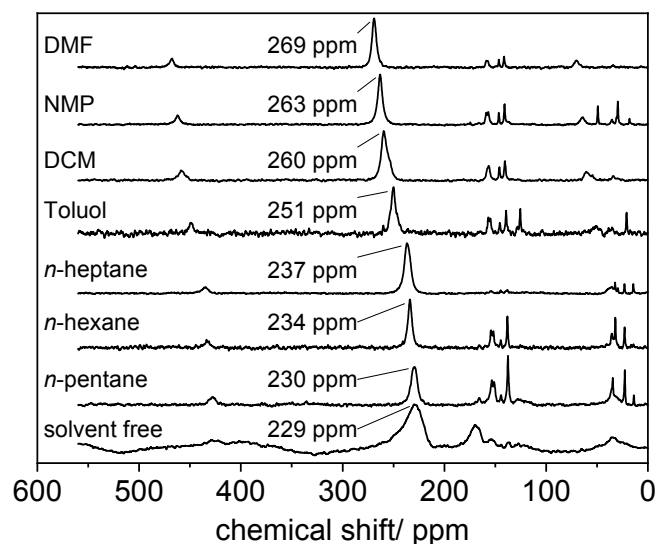
Figure S12. ^{13}C CP MAS NMR spectra of compound **1** soaked in different solvents.

The ^{1}H MAS NMR spectra (cf. Figure S13-S15) exhibit further interesting effects. First of all, a relatively broad signal centered at around 8 ppm is observed for the desolvated compound **1** which contains contributions from both, 2,6-ndc linkers and dabco (Figure S15). In samples loaded with unpolar solvents like *n*-heptane, the signal slightly shifts to 9 … 10 ppm and becomes narrower. The latter observation indicates that structure closing by desolvation results in a higher degree of local distortion around the protons giving rise to the line broadening compared to the more defined solvated state. For solvents of higher polarity such as DMF, a second major ^{1}H MAS NMR line (signal B) occurs at chemical shifts between ca. 12.5 and 13 ppm. Its intensity is comparable with that of the remaining signal A (see Figure 14). Taking into account the 2,6-ndc : dabco ratio of 2 : 1 in DUT-8(Ni) and the number of ^{1}H nuclei in in both molecules (6 in 2,6-ndc, 12 in dabco), it is tempting to speculate that these two signals are due to 2,6-ndc and dabco. In order to substantiate this speculation, we have synthesized the compounds **3**, **4**, and **5** using deuterated 2,6-ndc and/or dabco. The resulting ^{1}H MAS NMR spectra are shown in Figure S14. Deuteration of 2,6-ndc results in the disappearance of signal A and deuteration of dabco in the disappearance of signal B. In fully deuterated DUT-8(Ni), signals A and B disappear both. This clearly shows that signal A represents the 2,6-ndc linkers and signal B the dabco units in samples loaded with polar solvents. In samples loaded with unpolar solvents, 2,6-ndc and dabco contribute to signal A. Note, that partially deuterated samples (samples **3** and **4**) exhibit somewhat narrower ^{1}H MAS NMR signals than the fully protonated compound **1**. The likely reason for this observation is a reduced homonuclear magnetic dipole-dipole interaction among ^{1}H nuclei in the partially deuterated samples. It is well known that ^{1}H MAS NMR spectra often exhibit a line broadening due to the influence of this interaction[6] which can be reduced by partial deuteration. The assignment of signals A and B to 2,6-ndc and dabco, respectively could be confirmed by an ^{1}H-^{13}C HETCOR experiment (see Figure S16). At short mixing times, spin polarization is exchanged between closes neighbors only in this experiment. As can be seen in Figure S16, the dabco ^{13}C nuclei exchange spin polarization with ^{1}H nuclei at ca. 13 ppm in DMF and at ca. 10 ppm in n-heptane as expected from the above described observations.
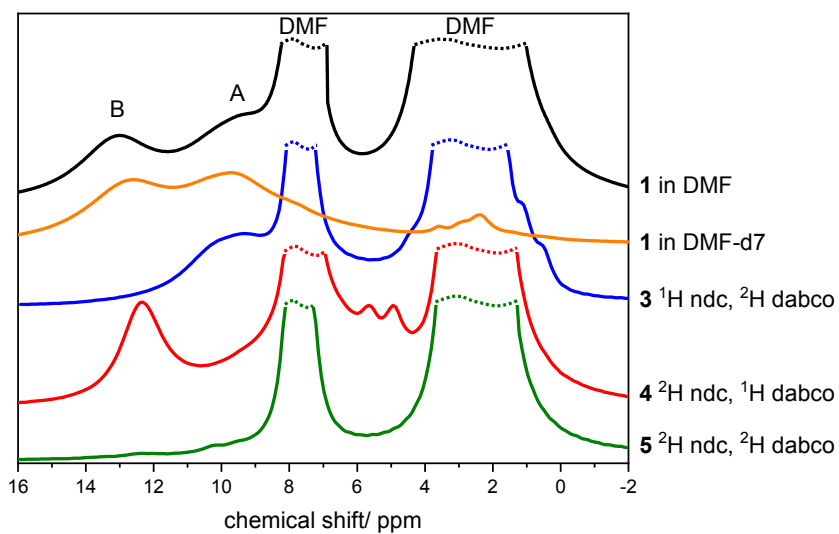
Figure S13. ^{1}H MAS NMR spectra of compound **1**, **3**, **4**, and **5** loaded with DMF and of compound **1** after solvent exchange by DMF-d7.
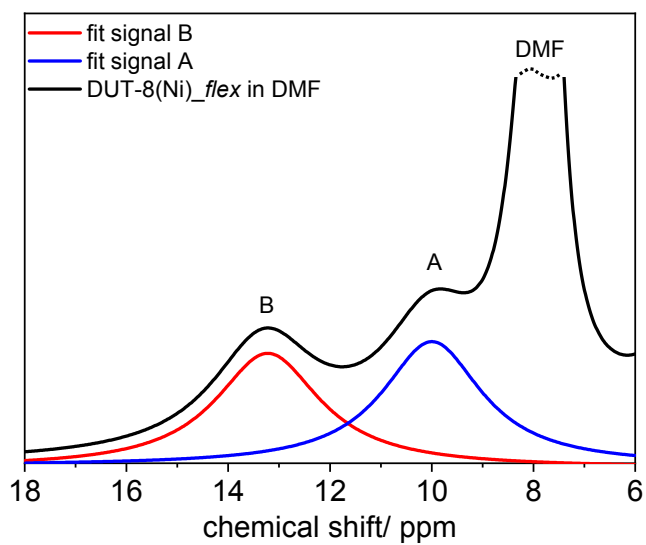

Figure S14. ^{1}H MAS NMR spectrum of compound **1** loaded with DMF and decomposition of the spectrum into signals A and B. Both signals are of comparable intensity within the experimental error.
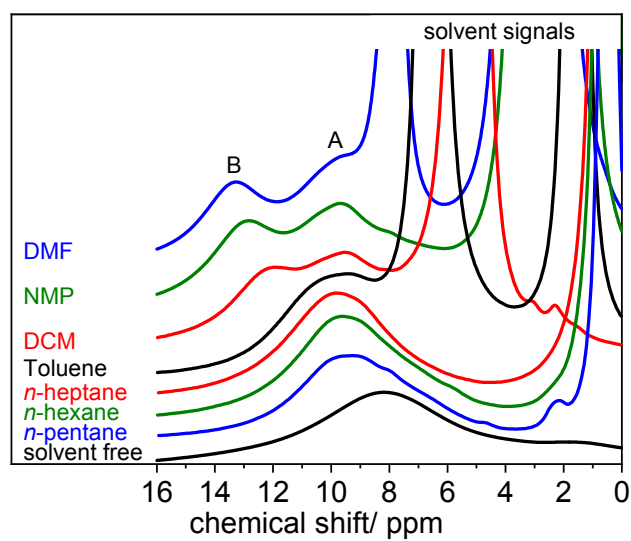
Figure S15. ^{1}H MAS NMR spectra of compound **1** soaked in different solvents. The intense solvent signals were cut to visualise the signals A and B due to the MOF.
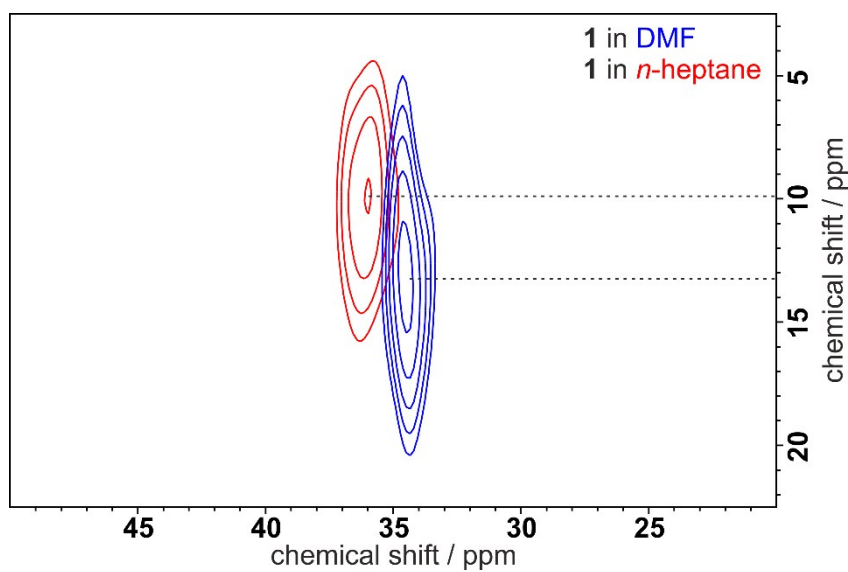

Figure S16. [1]H-^{13}C HETCOR spectrum of compound **1** solvated with DMF (blue) and *n*-heptane (red) measured at 350 µs contact time. Polarisation transfer then only takes place between closely neighboured ^{1}H and ^{13}C nuclei. For clarity, only the signal region of dabco at ca. 35 ppm for ^{13}C is shown.
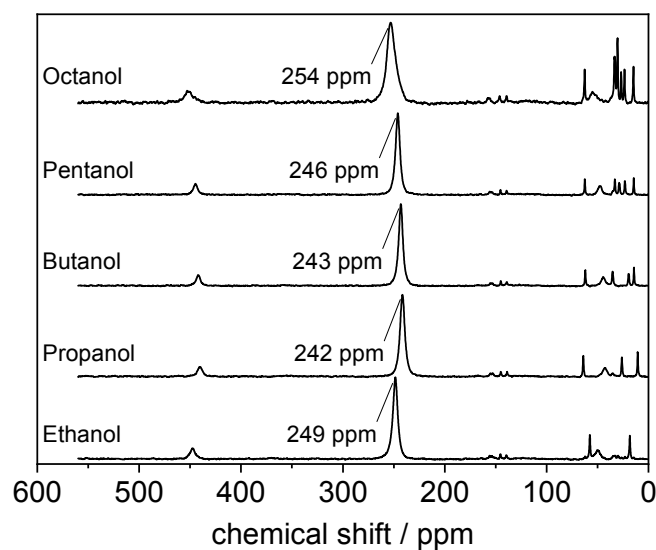
Figure S17. ^{13}C CP MAS NMR spectra of compound **1** soaked in different alcohols.

References

1.   M.M. Maricq and J.S. Waugh, *J. Chem. Phys.,* 1979, **70**, 3300.
2.   A. Nayeem and J. P. Yesinowski, *J. Chem. Phys.,* 1988, **89**, 4600.
3.   H. Liu, H.-M. Kao and C. P. Grey, *J. Phys. Chem. B,* 1999, **103**, 4786.
4.   N. Klein, C. Herzog, M. Sabo, I. Senkovska, J. Getzschmann, S. Paasch, M. R. Lohe, E. Brunner and S. Kaskel, *Phys. Chem. Chem. Phys.,* 2010, **12**, 11778.
5.   C. Reichardt and T. Welton, *Solvents and solvent effects in organic chemistry*, John Wiley & Sons, 2011.
6.   E. Brunner, D. Freude, B. C. Gerstein, and H. Pfeifer, *J. Magn. Reson.*, 1990, **90**, 90.